

On the efficiency of stochastic volume sources for the determination of light meson masses

E. Endress,¹ A. Jüttner,² and H. Wittig³

¹Instituto de Física Teórica UAM/CSIC, Facultad de Ciencias, Universidad Autónoma de Madrid, Cantoblanco, E-28049 Madrid, Spain

²CERN, Physics Department, TH Division, CH-1211 Geneva 23, Switzerland

³Institut für Kernphysik and Helmholtz Institute Mainz, Johannes Gutenberg-Universität Mainz, D-55009 Mainz, Germany

Abstract

We investigate the efficiency of single timeslice stochastic sources for the calculation of light meson masses on the lattice as one varies the quark mass. Simulations are carried out with $N_f = 2$ flavours of non-perturbatively $\mathcal{O}(a)$ improved Wilson fermions for pion masses in the range of 450 – 760 MeV. Results for pseudoscalar and vector meson two-point correlation functions computed using stochastic as well as point sources are presented and compared. At fixed computational cost the stochastic approach reduces the variance considerably in the pseudoscalar channel for all simulated quark masses. The vector channel is more affected by the intrinsic stochastic noise. In order to obtain stable estimates of the statistical errors and a more pronounced plateau for the effective vector meson mass, a relatively large number of stochastic sources must be used.

1 Introduction

In lattice QCD, hadronic properties such as masses and matrix elements can be computed in terms of Euclidean correlation functions. Typically, these are expectation values of properly selected polynomials in the quark and gluon fields that project on states with the desired quantum numbers. After performing the Wick contractions, correlation functions are expressed as traces over products of quark propagators, Dirac matrices and color-structures. In order to obtain precise estimates of hadron masses and transition amplitudes, variance reduction methods may be applied such that correlation functions with good statistical accuracy can be computed.

The quark propagator in coordinate space can be computed as the solution of the linear system

$$D\Phi = \eta, \tag{1}$$

where D is the lattice Dirac operator and η a source vector. In its simplest form, η is taken to be a point source, i.e.¹

$$\eta(x') = \delta_{x'y}. \tag{2}$$

This implies that the solution of eq. (1) yields the quark propagator from a single point y to any other point x , which corresponds to just one column of the propagator matrix. Thanks to translational invariance a large class of correlation functions can be defined in terms of these “one-to-all” propagators. However, in this way only a small fraction of the information contained in D is processed. In typical simulations of lattice QCD the sparse matrix D has $O(10^9 \times 10^9)$ entries, and solving eq. (1) to machine precision for all source positions is therefore beyond the capabilities of even the most powerful supercomputers. Volume-filling random-noise sources have been proposed as a means to access the full propagator matrix [1–4] by replacing it with a stochastic estimate. These stochastic “all-to-all” propagators have been successfully applied in a number of different contexts [2–11, 14, 15]. However, care must be exercised in their actual construction, since an arbitrarily chosen stochastic source vector can induce a large variance into hadronic correlation functions. In other words, for the method to be efficient, one must ensure that the intrinsic stochastic noise does not overwhelm the gain in information provided by having access to the entire propagator matrix. A particular technique, which proved to be quite efficient, is the so-called “one-end trick”, pioneered in [5, 9] and successfully applied in several studies of light meson physics [10, 11, 14, 15].

In this article we present a systematic study of the effectiveness of single-timeslice stochastic sources. In particular, we monitor the variance and the computational cost as a function of the quark mass and compare it to the variance achieved with point sources. Our simulations are performed for QCD with $N_f = 2$ flavours of $O(a)$ improved Wilson quarks. We concentrate on two-point correlation functions of the pion and the rho meson.

The outline of this paper is as follows: in section 2 we revisit the concepts of stochastic volume sources and the one-end trick. The set-up of our simulations is discussed in section 3, and our main results are presented in section 4. Finally, section 5 contains a summary of our findings as well as some concluding remarks.

¹For simplicity we suppress colour and spinor indices.

2 Stochastic propagator estimation

In this paper we restrict ourselves to two-point correlation functions of a flavour off-diagonal quark bilinear, $O_{ud}(x) = \bar{u}(x)\Gamma d(x)$, where u and d denote the fields of the up- and the down-quarks, respectively, and Γ is one of the 16 Dirac matrices specifying the desired quantum number. The two-point correlation function is given by

$$\langle \mathcal{O}_{ud}(x)\mathcal{O}_{ud}^\dagger(y) \rangle = \langle \text{Tr} \left\{ S(x,y)\Gamma S(y,x)\tilde{\Gamma} \right\} \rangle, \quad (3)$$

where $\tilde{\Gamma} = \gamma_0\Gamma^\dagger\gamma_0$, and $\langle \dots \rangle$ denotes the average over the gauge configurations. Since we assume exact isospin symmetry, the same symbol, S , is used to denote the propagator for both quark flavours. The spectrum of the particles with the prescribed quantum numbers can then be determined from the exponential decay of the zero-momentum projection, i.e.

$$C_2(t; y) = \sum_{\vec{x}} \langle \text{Tr} \left\{ S(x,y)\Gamma S(y,x)\tilde{\Gamma} \right\} \rangle, \quad t = x_0 - y_0. \quad (4)$$

For a given gauge field the propagator $S(x,y)$ from lattice sites y to x , is obtained as the solution of the linear system²

$$\sum_z \sum_{c,\gamma} D_{\alpha\gamma}^{ac}(x,z)S_{\gamma\beta}^{cb}(z,y) = \delta_{\alpha\beta}\delta^{ab}\delta_{xy}. \quad (5)$$

Using point sources amounts to solving the linear system for one particular choice of y . This implies that altogether 12 inversions must be performed, since four spinor and three colour components must be considered independently. While this is sufficient to compute the correlation function $C_2(t; y)$, the statistical signal could be further improved by averaging over many different source points. An improved estimator for the correlation function is obtained by

$$\tilde{C}_2(t) \equiv \frac{1}{V_3} \sum_{\vec{y}} C_2(t; y) = \frac{1}{V_3} \sum_{\vec{x}, \vec{y}} \langle \text{Tr} \left\{ S(x,y)\Gamma S(y,x)\tilde{\Gamma} \right\} \rangle, \quad t = x_0 - y_0, \quad (6)$$

where V_3 denotes the number of lattice sites within one timeslice. In order to see how such an average can be effected, we revisit the method of stochastic noise sources in the following.

2.1 General stochastic noise sources

In the stochastic approach, an ensemble of N_r random vectors, $\{\eta^{(r)}(x_0, \vec{x}) | r = 1, \dots, N_r\}$, is generated for each gauge configuration. The number N_r is sometimes referred to as the number of ‘‘hits’’. These source vectors are created by assigning independent random numbers to all components, i.e. to all lattice sites, colour and Dirac indices. Each random number is drawn from a distribution \mathcal{D} which is symmetric about zero in the hit limit $N_r \rightarrow \infty$, i.e.

$$\langle \eta_\alpha^a(x_0, \vec{x}) \rangle_{\text{src}} \equiv \lim_{N_r \rightarrow \infty} \frac{1}{N_r} \sum_{r=1}^{N_r} (\eta^{(r)})_\alpha^a(x_0, \vec{x}) = 0. \quad (7)$$

In addition the sources satisfy

$$\langle \eta_\alpha^a(\vec{x}, x_0)(\eta^\dagger)_\beta^b(\vec{y}, y_0) \rangle_{\text{src}} = \delta_{x_0 y_0} \delta_{\vec{x}\vec{y}} \delta_{\alpha\beta} \delta^{ab}. \quad (8)$$

² Latin indices are used to label color, while Greek letters denote spinor components.

Solving the linear system of eq. (1) for each of the N_r source vectors yields a set of solution vectors

$$(\Phi^{(r)})_\alpha^a(x) = \sum_z \sum_{c,\gamma} S_{\alpha\gamma}^{ac}(x, z) (\eta^{(r)})_\gamma^c(z). \quad (9)$$

The estimate of the entire propagator is defined as the stochastic average (“hit average”) over the product between solution and noise vectors

$$\left\langle \Phi_\alpha^a(x) (\eta^\dagger)_\beta^b(y) \right\rangle_{\text{src}} = \sum_z \sum_{c,\gamma} S_{\alpha\gamma}^{ac}(x, z) \delta_{zy} \delta_{\gamma\beta} \delta^{cb} = S_{\alpha\beta}^{ab}(x, y). \quad (10)$$

It remains to specify the distribution from which the random vectors $\eta^{(r)}$ are drawn. In refs. [1,2] it was noted that a flat distribution of $\mathbb{Z}(2)$ -elements, $(\eta^{(r)})_\alpha^a(x) \in \mathcal{D} = \mathbb{Z}(2) = \{+1, -1\}$, or, more generally, elements of $\mathcal{D} = \mathbb{Z}(N)$ is very effective in realising the condition of eq. (8). In this work we follow Foster and Michael [5] and draw separate elements of $\mathbb{Z}(2)$ for the real and imaginary parts of the source vector, i.e.

$$\mathcal{D} = \mathbb{Z}(2) \otimes \mathbb{Z}(2) = \left\{ \frac{1}{\sqrt{2}} (\pm 1 \pm i) \right\}. \quad (11)$$

Experience shows that a random source vector, which is distributed over the entire space-time lattice, leads mostly to a very noisy signal for hadronic correlation functions. An essential step towards a significant variance reduction is taken by restricting the support of the source vector to individual timeslices, Dirac or colour components [8]. Such “dilution schemes”, and, in particular, the so-called time-dilution are widely used in the computation of hadronic properties [5,7,8]. Here, the non-zero components of the random source vector are restricted to a single timeslice, e.g. $y_0 = 0$

$$\eta(y) = \begin{cases} \tilde{\eta}(\vec{y}), & \text{if } y_0 = 0, \\ 0, & \text{otherwise} \end{cases}. \quad (12)$$

We end this discussion with a few general remarks. In practice the limit $N_r \rightarrow \infty$ cannot be taken, and thus the details of constructing the random source should be optimized for the correlation function at hand. In ref. [11] it was noted that for many correlators the stochastic and gauge averages commute. It then suffices to generate a reasonably small number of random source vectors per gauge configuration, since the ensemble average automatically implies the stochastic average.

2.2 The one-end trick revisited

The naive implementation of stochastic sources consists in replacing each propagator in the correlation function of eq. (6) by the stochastic estimate of eq. (10). For a general choice of Γ this implies that an independent source vector must be used for each quark propagator, in particular if Γ couples different Dirac components. This typically results in a relatively noisy signal [12]. By contrast, for correlators which involve only diagonal combinations of spinor components, it is possible to compute the two-point function stochastically using only a single random source, which is distributed over all colour and Dirac components within one timeslice. The relative numerical effort compared to using a point source is thereby reduced by a factor 12 per hit: Setting $N_r = 12$ results in the same number of inversions that must

be performed, while the statistical error can be expected to be reduced. This is the so-called “one-end trick” [5, 9].

The situation in the case of correlation functions, in which different spinor components are coupled, is less favourable but can be dealt with via the generalized one-end trick, sometimes also referred to as the “linked source method” [14]. It amounts to choosing a spin-diagonal random source vector, which has support only for a particular spin component τ and a single timeslice y_0 (e.g. $y_0 = 0$), viz.

$$(\eta^{(r)})_{\sigma}^b(y) = (\xi^{(r)})^b(\vec{y}) \delta_{0y_0} \delta_{\sigma\tau}, \quad (13)$$

where the components of the stochastic vector $\xi^{(r)}$ are drawn from a distribution \mathcal{D} and satisfy

$$\left\langle \xi^a(\vec{x})(\xi^\dagger)^b(\vec{y}) \right\rangle_{\text{src}} = \delta_{\vec{x}\vec{y}} \delta^{ab}. \quad (14)$$

Solving the linear system of eq. (1) for spin component τ yields the solution vector $\Phi(x)$, i.e.

$$(\Phi^{(r)})_{\alpha;\tau}^a(x) = \sum_{\vec{y}} \sum_b S_{\alpha\tau}^{ab}(x, y)|_{y_0=0} \xi^b(\vec{y}). \quad (15)$$

The correlation function at zero momentum is then obtained as

$$\tilde{C}_2(t) = - \left\langle \sum_{\vec{x}} \sum_{a,\alpha,\tau} \left\langle \left[(\Gamma\gamma_5)\Phi(x)^\dagger \right]_{\tau;\alpha}^a \left[(\gamma_5\tilde{\Gamma})\Phi(x) \right]_{\tau;\alpha}^a \right\rangle_{\text{src}} \right\rangle, \quad (16)$$

which is the stochastic estimator of the two-point function at zero momentum of eq. (6) after applying eq. (8). The generalized one-end trick can be applied whenever the stochastic source vector commutes with the given choice of Γ -matrices. The spin-diagonal source vector $\xi^{(r)}$ satisfies this requirement by construction. Compared with the point source, the numerical effort is reduced by a factor three per hit.

The use of linked sources is not mandatory for pseudoscalar mesons, since the diagonal Γ -structure of the associated correlators ($\Gamma\gamma_5 = 1$) implies that stochastic noise vectors commute without any modification. However, during the course of a simulation, many different hadronic channels, involving arbitrary Dirac structures at both the source and sink, are considered. In order to facilitate the cost comparison for different correlator channels, we have implemented linked sources by default, and below we proceed to compare their effectiveness in simulations covering a range of light quark masses for both the pseudoscalar and vector channel. According to ref. [11], the use of linked sources for pseudoscalar mesons was not found to be inferior compared with non spin-diagonal sources, at fixed computational cost.

One potential drawback of the one-end trick is that two-point functions cannot be computed for arbitrary momenta using a given set of noise vectors. Owing to the automatic summation over the spatial source and sink coordinates, a specific momentum is selected. To utilize the one-end trick for computing the two-point correlator at a given non-zero momentum, the set of noise vectors $\{\eta^{(r)}(y_0, \vec{y}) | r = 1, \dots, N_r\}$ must be transformed separately for each selected momentum with an appropriate phase $e^{i\vec{p}\vec{y}}$ prior to performing the inversion. It is worth noting that (partially) twisted boundary conditions [13] can be successfully combined with random sources [14, 16]. Again, for each momentum channel, N_r extra inversions are then required, and thus the numerical cost increases in relation to the point source, where the two-point function can be projected at least on the Fourier modes at negligible additional cost.

3 Simulation setup

This work is based on gauge configurations with $N_f = 2$ flavours of non-perturbatively $O(a)$ -improved Wilson fermions which have been generated as part of the CLS effort [17], using the deflation-accelerated DD-HMC algorithm [18]. This algorithm combines domain-decomposition (DD) methods [19] with the Hybrid Monte Carlo (HMC) algorithm [20] and the Sexton-Weingarten multiple-time integration scheme [21]. All ensembles in this work were generated for $\beta = 5.3$, a choice for which the coefficient of the Sheikholeslami-Wohlert term was determined as $c_{\text{sw}} = 1.90952$ [22].

| Run | Lattice | Number cfs. | κ_{sea} | am_π | m_π [MeV] |
|-------|------------------|-------------|-----------------------|-------------|---------------|
| E_2 | 64×32^3 | 158 | 0.13590 | 0.24292(29) | 760 |
| E_3 | 64×32^3 | 156 | 0.13605 | 0.20645(37) | 645 |
| E_4 | 64×32^3 | 162 | 0.13610 | 0.19305(41) | 605 |
| E_5 | 64×32^3 | 159 | 0.13625 | 0.14345(55) | 450 |

Table 1: Simulation parameters and pion masses. The latter are determined using the one-end-trick with $N_r = 6$ hits each on three different timeslices for the source vector.

Our simulation parameters are listed in Table 1. The ensembles contain configurations which are sufficiently separated in Monte Carlo time such that autocorrelations can be safely ignored. In this work we always set the valence quark mass equal to that of the sea quarks. The inversions of the Wilson-Dirac operator of eq. (1) were performed using a Schwarz-preconditioned generalized conjugate residual (SAP+GCR) algorithm [23]. Further simulation details are described in [24]. The conversion of pion masses into physical units was performed using the preliminary scale determination via the mass of the Omega baryon [25], which yields $a = 0.063$ fm at $\beta = 5.3$.

Mesonic two-point correlators were computed in the pion ($\Gamma = \gamma_5$) and rho ($\Gamma = \gamma_i$) channels. For the latter we averaged the contributions from all three spatial γ -matrices. Only flavour non-singlet correlators were considered. The quark propagators entering the correlation functions were computed either using a point source or by applying a random source in the manner of the generalized one-end trick described above. For the latter linked sources with $N_r = 1, 3$ and 6 hits were used. While for $N_r = 3$ hits the numerical effort expressed in terms of the number of inversion remains the same as for the point source, it reduces by a factor of three for $N_r = 1$. Six hits represent twice as many inversions compared to the point source. In order to study the scaling of the variance with N_r in a more detailed manner, we used as many as 25 hits for ensemble E_4 . The accuracy of our calculations is enhanced by averaging the results obtained for three different locations for each type of source, corresponding to source positions $x_0/a = 0, 21$ and 42.

In our analysis the forward-backward symmetry of the correlators was exploited to average the data about the central timeslice $T/2$. In order to extract the masses of the ground state we performed correlated χ^2 -minimizing fits to the folded correlation functions. The next-to-lowest state was explicitly taken into account, by substituting its energy by $3m_\pi$ in the pseudoscalar channel and $2\sqrt{m_\pi^2 + (2\pi/L)^2}$ in the vector channel, respectively [26]. Statistical errors were determined via the single-elimination jackknife method. As will be explained below, the achieved statistical precision on spectral quantities enters our definition

of a measure for the efficiency of stochastic sources. In order to quantify the significance of this measure we have used Berg’s proposal [27] of a nested jackknife procedure (also referred to as second-level jackknife) to estimate the fluctuations of the statistical error (i.e the “error of the error”).

4 Results: Pseudoscalar and vector meson two-point correlators

Our objective is to compare the performance of point sources and the generalized one-end trick when computing light meson masses. Therefore, for a variety of different quark masses the resulting variances are monitored as a function of the computational effort, which is expressed in terms of the number of inversions, N_{inv} , which are required to solve the linear system of eq. (1) for one particular source position. This is motivated by the observation that the number of iterations of the deflated SAP+GCR solver does not depend on the source type but only on the simulated quark mass. Note that N_{inv} represents the number of inversions per source position.

Table 2 contains the results of the pion and rho meson mass fits using both source types for the various gauge field ensembles whose simulation parameters are listed in Table 1. By default, results from the three source positions are averaged over. The results are illustrated in Fig. 1, which shows the ratio of errors obtained using stochastic volume sources and point sources, respectively.

| Source type | N_{inv} | E_2 | E_3 | E_4 | E_5 |
|----------------|------------------|-------------|-------------|-------------|-------------|
| am_π | | | | | |
| Point | 12 | 0.24216(52) | 0.20647(52) | 0.19240(69) | 0.14264(81) |
| Volume: 1 hit | 4 | 0.24337(35) | 0.20684(45) | 0.19335(47) | 0.14402(59) |
| Volume: 3 hits | 12 | 0.24309(30) | 0.20650(40) | 0.19320(42) | 0.14346(57) |
| Volume: 6 hits | 24 | 0.24292(29) | 0.20645(37) | 0.19305(41) | 0.14345(55) |
| am_ρ | | | | | |
| Point | 12 | 0.3782(38) | 0.3501(49) | 0.3353(56) | 0.2842(80) |
| Volume: 1 hit | 4 | 0.3819(57) | 0.3523(80) | 0.3166(80) | 0.2909(139) |
| Volume: 3 hits | 12 | 0.3843(39) | 0.3518(52) | 0.3367(54) | 0.2820(73) |
| Volume: 6 hits | 24 | 0.3858(29) | 0.3559(39) | 0.3333(36) | 0.2842(61) |

Table 2: Pion (upper half) and rho meson (lower half) masses computed using point sources and the generalized one-end trick with $N_r = 1, 3$ and 6 hits for the ensembles $E_2 - E_5$. N_{inv} denotes the number of inversions per source position. Fit ranges were chosen as $10 \leq x_0/a \leq 30$ and $11 \leq x_0/a \leq 30$ in the pion and rho meson channels, respectively. In case of the lightest rho meson the fit range was reduced to $11 \leq x_0/a \leq 27$, due to strong fluctuations around the central timeslice.

Our investigation of the uncertainty in the statistical error estimate itself via a nested jackknife procedure revealed that the fluctuations in the error estimate are quite small, amounting on average to about (4 – 7)% in the pion channel and (7 – 10)% in the rho meson channel, respectively.

Comparing the conventional point source to the generalized one-end trick in the pion channel we observe that random noise sources lead to a considerable improvement of the

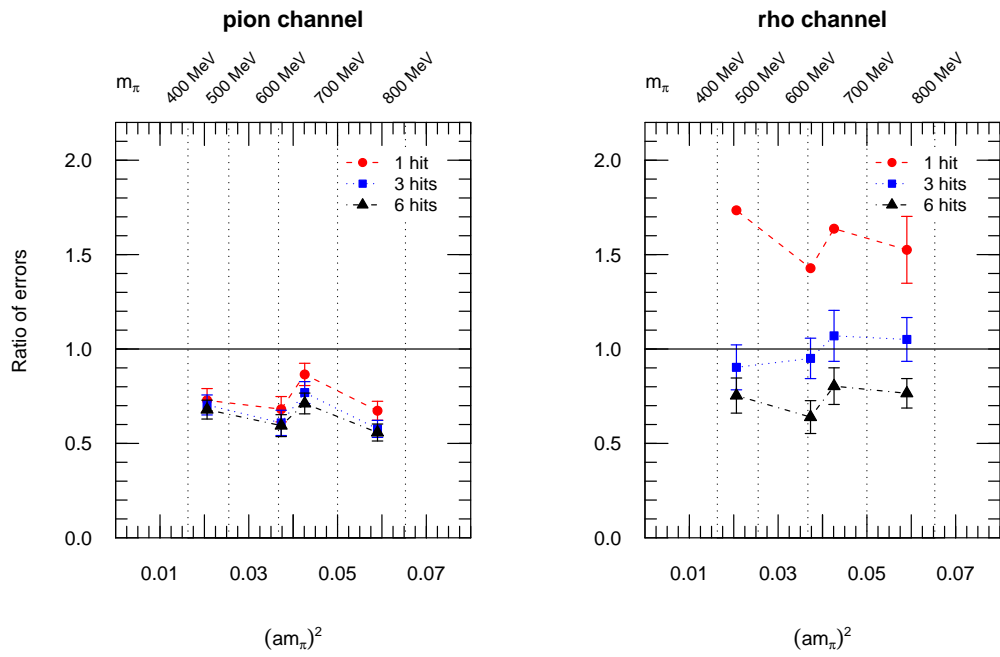


Figure 1: The statistical error of meson masses computed using volume sources normalized by the error obtained with the point source, plotted against the squared pion mass for $N_T = 1, 3$ and 6 hits. Error bars (where shown) were obtained using a nested jackknife procedure.

| hits | N_{inv} | E_4 | | hits | N_{inv} | E_4 | |
|------|------------------|-------------|------------|------|------------------|-------------|------------|
| | | am_π | am_ρ | | | am_π | am_ρ |
| pt | 12 | 0.19240(69) | 0.3353(56) | 8 | 32 | 0.19302(41) | 0.3370(35) |
| 1 | 4 | 0.19335(47) | 0.3166(80) | 9 | 36 | 0.19304(41) | 0.3361(34) |
| 2 | 8 | 0.19326(44) | 0.3352(67) | 10 | 40 | 0.19299(41) | 0.3363(33) |
| 3 | 12 | 0.19320(42) | 0.3367(54) | 13 | 52 | 0.19291(41) | 0.3377(32) |
| 4 | 16 | 0.19300(42) | 0.3288(43) | 16 | 64 | 0.19286(40) | 0.3399(29) |
| 5 | 20 | 0.19302(42) | 0.3328(41) | 19 | 76 | 0.19289(40) | 0.3408(29) |
| 6 | 24 | 0.19305(41) | 0.3333(36) | 22 | 88 | 0.19291(40) | 0.3417(28) |
| 7 | 28 | 0.19301(41) | 0.3346(34) | 25 | 100 | 0.19293(40) | 0.3430(27) |

Table 3: Variance reduction of the generalized one-end trick as a function of the number of hits. Pion and rho meson masses for $N_r = 1, \dots, 25$ hits computed on the ensemble E_4 . The values of the point source (labeled by 'pt') are taken from Table 2.

statistical signal. Already a single random noise vector, corresponding to one third of the relative computational effort leads to a significantly reduced variance. The variance saturates very quickly when increasing the number of hits. This implies that the gauge noise dominates over the stochastic noise of random volume sources. Furthermore, a considerable improvement of at least 25 percent at equal cost is observed for all simulated quark masses. Our confidence in the results is supported by the quality of plateaus of effective masses. The plots for the pion are shown in Fig. 5 of Appendix A and illustrate that outliers of the plateau are suppressed due to the volume averaging effect of our stochastic sources.

In the vector channel the generalized one-end trick is less effective. A single hit does not suffice to reach the precision of the point source method and no reliable estimates for the errors of the error were obtained. Therefore, in the right panel of Fig. 1 the errorbars of the results of a single hit are suppressed for small quark masses. However, at equal computational cost the variances are comparable and, in particular, for the two lightest quark masses the volume source slightly gains over the conventional point source. Contrary to the pion channel, it is seen that the stochastic noise is not immediately saturated and increasing the number of hits reduces the variance significantly.³ In order to study the scaling of the variance in more detail we have computed the pseudoscalar and vector correlators on the E_4 ensemble for up to 25 hits. The results are shown in Table 3 and Fig. 2.

The results compiled in the table demonstrate that the variance in the pion channel is saturated already after performing three hits, indicating that this correlator is dominated by the gauge noise. Increasing N_r from 3 to 25 results in a small additional reduction of the error in the pion mass of only about 5%.

By contrast, the stochastic noise dominates in the rho meson channel. Increasing N_r from 1 to 7 produces a reduction of the statistical error by 60%, and a further 10% can be gained if N_r is as large as 25. Assuming that the error scales like $\mathcal{O}(1/\sqrt{N_r})$, one expects that the squared error times the number of inversions N_r is constant. As the right panel in Fig. 2 shows quite clearly, this is indeed true in the vector channel for $N_r \lesssim 7$. When larger values of N_r are considered, the rate of error reduction slows down relative to the extra number of inversions, and thus the procedure becomes increasingly ineffective in terms of computational

³The effective mass plots of the rho meson are shown in Fig. 6 of Appendix B.

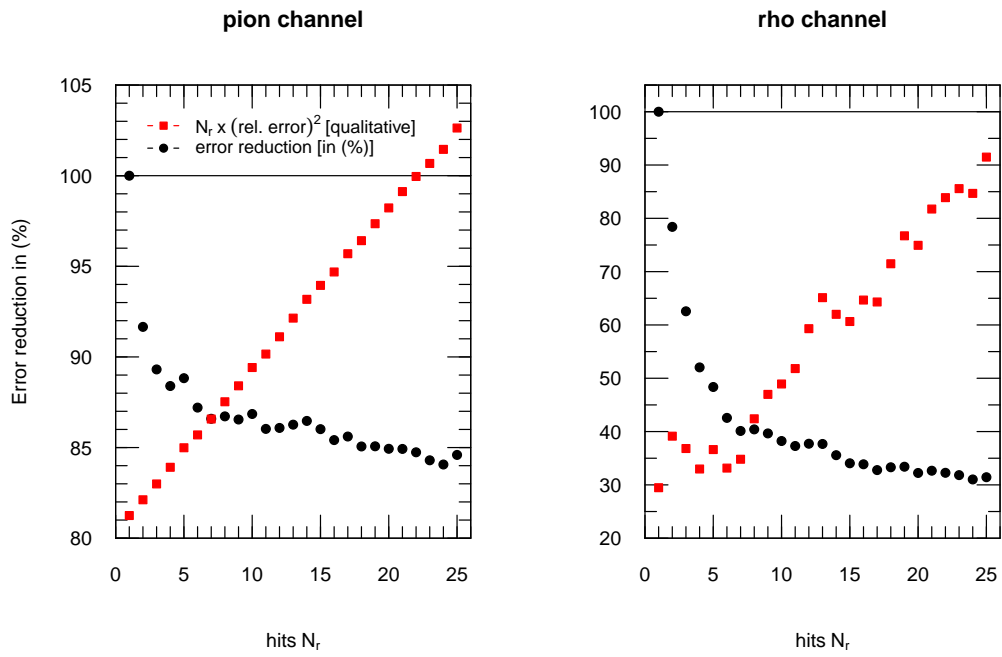


Figure 2: Effectiveness of stochastic sources as a function of the number of hits, N_r , for ensemble E_4 in the pseudoscalar (left panel) and vector (right panel) channels. Solid black points represent the statistical error relative to the single-hit volume source. Red squares denote the variance scaled by the number of hits.

| | point | $N_r = 3$ | $N_r = 6$ | $N_r = 9$ | $N_r = 16$ |
|------------|-------|-----------|-----------|-----------|------------|
| point | 0 | 0.08 | 0.21 | -0.10 | -0.30 |
| $N_r = 3$ | -0.07 | 0 | 0.13 | -0.16 | -0.35 |
| $N_r = 6$ | -0.17 | -0.11 | 0 | -0.25 | -0.42 |
| $N_r = 9$ | 0.11 | 0.19 | 0.34 | 0 | -0.23 |
| $N_r = 16$ | 0.43 | 0.54 | 0.73 | 0.29 | 0 |

Table 4: The relative efficiency ϵ_{ij} in the vector channel for ensemble E_4 .

overhead.

In order to formulate a more quantitative criterion for the performance of point and stochastic sources, we define the relative efficiency, ϵ_{ij} , of two procedures i and j , as

$$\epsilon_{ij} := \frac{[(\text{variance}) \times (\text{number of inversions})]_i}{[(\text{variance}) \times (\text{number of inversions})]_j} - 1. \quad (17)$$

Thus, the ratio of the squared error is scaled with the ratio of the computational cost. In Table 4 we list the values for ϵ_{ij} in the vector channel for ensemble E_4 . The information in this matrix-like table must be interpreted in the following way: a negative entry ϵ_{ij} in row i and column j means that procedure i is more efficient than j by $(100 \times |\epsilon_{ij}|)\%$. From the numbers in Table 4 one concludes that, in the vector channel, a volume source with $N_r = 3$ is only slightly more efficient than the point source, even though the number of inversions performed in both cases is the same. However, if one demands that the statistical error be at least as small as for the point source, a larger number of hits is more favourable: According to Table 3, $N_r = 6$ seems to be the optimal choice, since the extra numerical effort is more than compensated by the resulting reduction in the variance.

In Fig. 3 the relative efficiency defined in eq. (17) with respect to the point source is plotted as a function of the squared pion mass. For a single hit the volume source is about a factor of five more efficient than the point source in the pion channel whereas at identical computational cost the volume source still outperforms the point source by a factor of two. As pointed out before, this loss of efficiency is due to the fact that in the pion channel the variance is completely dominated by the gauge noise. The gain in the vector channel is not so obvious. A stochastic volume source with $N_r = 6$ hits appears to be a good compromise between numerical effort and statistical accuracy across the entire mass range under study, despite the large uncertainties in the relative efficiency ϵ_{ij} in the vector channel (see Figs. 1 and 3).

Another beneficial effect of using random sources in the vector channel can be seen from the effective mass plot shown in Fig. 4. By comparing the data obtained using $N_r = 6$ and $N_r = 25$ hits with those of the point source, one clearly sees that not only the statistical error decreases for a large hit number but that the overall quality of the plateau is much improved as well. This should make for much more reliable estimates of the mass in the vector channel.

Finally we investigate the effects on the variance of distributing random noise sources on several timeslices instead of placing them on a single one. Let N_{tot} denote any number of inversions of the Dirac operator. If the random noise source is placed on N_{ts} different timeslices, and if N_r hits are performed for each of these source positions, then $N_{\text{tot}} = N_{\text{ts}} \cdot N_r$. Can the variance be reduced by choosing N_{ts} and N_r such that N_{tot} stays fixed?

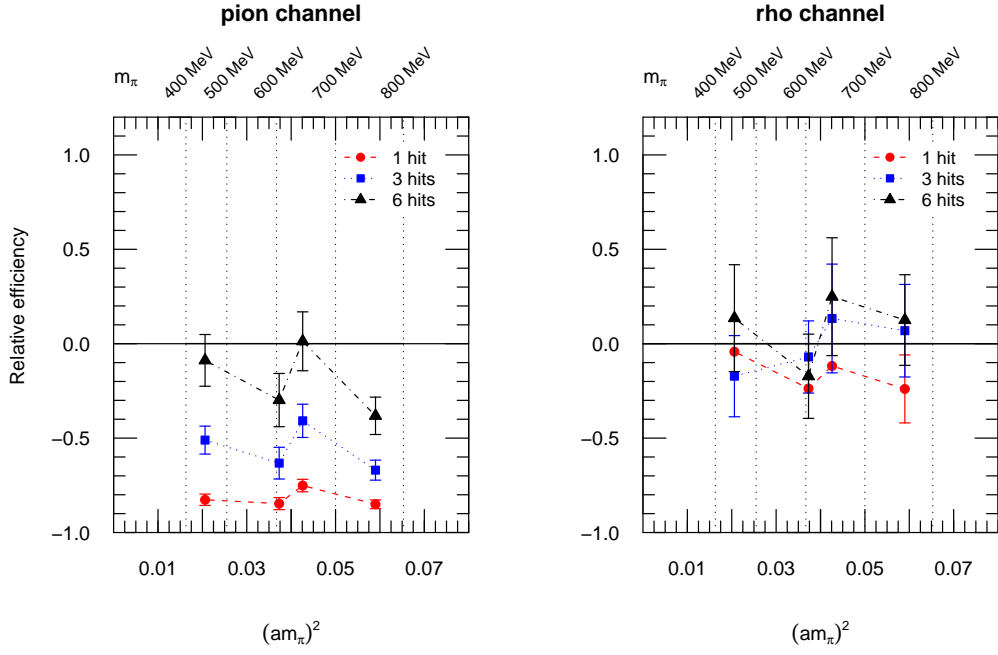


Figure 3: Relative efficiency as defined in eq. (17) with respect to the point source as a function of the squared pion mass for the pion (left panel) and rho meson (right panel) using $N_r = 1, 3$ and 6 hits.

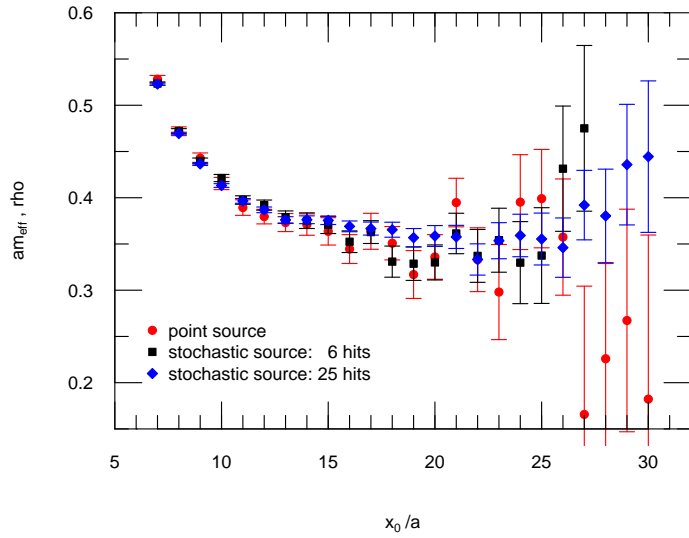


Figure 4: Effective masses in the vector channel obtained by means of the point source and random sources with 6 and 25 hits.

| | N_r | $N_{ts} = 1$ [0] | N_r | $N_{ts} = 2$ [0,21] | N_r | $N_{ts} = 3$ [0,21,42] |
|-----------|-------|------------------|-------|---------------------|-------|------------------------|
| am_π | 3 | 0.19327(58) | | | 1 | 0.19335(47) |
| | 6 | 0.19315(55) | 3 | 0.19330(49) | 2 | 0.19326(44) |
| | 9 | 0.19303(54) | | | 3 | 0.19320(42) |
| | 12 | 0.19296(53) | 6 | 0.19314(47) | 4 | 0.19300(42) |
| | 15 | 0.19297(54) | | | 5 | 0.19302(42) |
| | 18 | 0.19304(54) | 9 | 0.19306(46) | 6 | 0.19305(41) |
| | 21 | 0.19307(54) | | | 7 | 0.19301(41) |
| | 24 | 0.19308(54) | 12 | 0.19293(46) | 8 | 0.19302(41) |
| am_ρ | 3 | 0.3290(89) | | | 1 | 0.3166(80) |
| | 6 | 0.3268(59) | 3 | 0.3303(59) | 2 | 0.3352(67) |
| | 9 | 0.3259(50) | | | 3 | 0.3367(54) |
| | 12 | 0.3285(48) | 6 | 0.3265(42) | 4 | 0.3288(43) |
| | 15 | 0.3329(45) | | | 5 | 0.3328(41) |
| | 18 | 0.3366(44) | 9 | 0.3308(40) | 6 | 0.3333(36) |
| | 21 | 0.3387(45) | | | 7 | 0.3346(34) |
| | 24 | 0.3429(44) | 12 | 0.3349(36) | 8 | 0.3370(35) |

Table 5: Comparison of effective masses in the pion (upper half) and rho (lower half) channels, averaged over N_{ts} different source positions which are indicated in the square brackets. N_r denotes the performed number of hits per source position. The total number of inversions, $N_{tot} = N_{ts} \cdot N_r$, is constant in each row of the table.

The results of such an analysis are shown in Table 5. Each row represents a particular fixed value of N_{tot} . In the pion channel there are clear indications that the statistical error decreases when more timeslices are used. In the vector channel this effect is less pronounced but becomes evident when $N_{ts} \cdot N_r \gtrsim 12$. Thus, a good strategy to enhance that statistical accuracy of mesonic two-point correlation functions is to use as many timeslices as one can afford for a fixed total number of inversions.

5 Summary and conclusions

In this paper we have presented a systematic study of random noise sources for the calculation of mesonic two-point correlation functions, using $O(a)$ improved Wilson fermions as our discretization. Specifically, we have investigated the effectiveness of the generalized one-end trick in the pseudoscalar and vector channels, for pion masses ranging from 450 to 760 MeV. Our spatial volumes correspond to a box length of $L = 2$ fm. The total number of inversions of the lattice Dirac operator serves as our measure for the computational cost.

Our findings are best summarized by a list of empirical observations:

- At equal computational cost, stochastic volume sources significantly enhance the statistical accuracy of correlation functions in the pseudoscalar channel. Here the signal is dominated by fluctuations in the gauge configurations, and the extra noise introduced by the stochastic procedure is rapidly suppressed.
- Stochastic volume sources help to stabilize mass estimates in the vector channel. In addition to reducing the variance, stochastic volume sources also produce a more pronounced plateau in the effective mass plot. Compared to the pion channel, however, a larger number of hits must be performed, before the improvement is clearly visible. In order to observe a clear advantage over ordinary point sources in our studied mass range, the numerical effort must at least be doubled for the generalized one-end trick.
- For fixed numerical cost, the quality of mesonic two-point correlation functions computed using random volume sources can be improved by averaging over several source positions, $N_{ts} > 1$, and adjusting the number of hits, N_r , such as to keep the total number of inversions fixed. In other words, averaging over more source positions is more effective in reducing the variance than increasing the number of hits.

The use of random volume sources is an attractive method, designed to extract more information on hadronic properties from the full propagator matrix at reasonable cost. It is particularly useful if the number of available gauge configurations is relatively small. Given the convincing performance reported here for the simple case of mesonic two-point functions, we have employed random noise sources in our projects to determine the electromagnetic pion form factor and the form factors for $K_{\ell 3}$ decays [28].

Acknowledgments

We thank our colleagues participating in the CLS project for sharing gauge ensembles. Calculations of correlation functions were performed on the "Hydra" cluster at the IFT, University of Madrid and the dedicated QCD platform "Wilson" at the Institute for Nuclear Physics, University of Mainz. E.E. is supported by the Research Executive Agency (REA) of the European Union under Grant Agreement PITN-GA- 2009-238353 (ITN STRONGnet).

A Effective mass plots: pseudoscalar channel

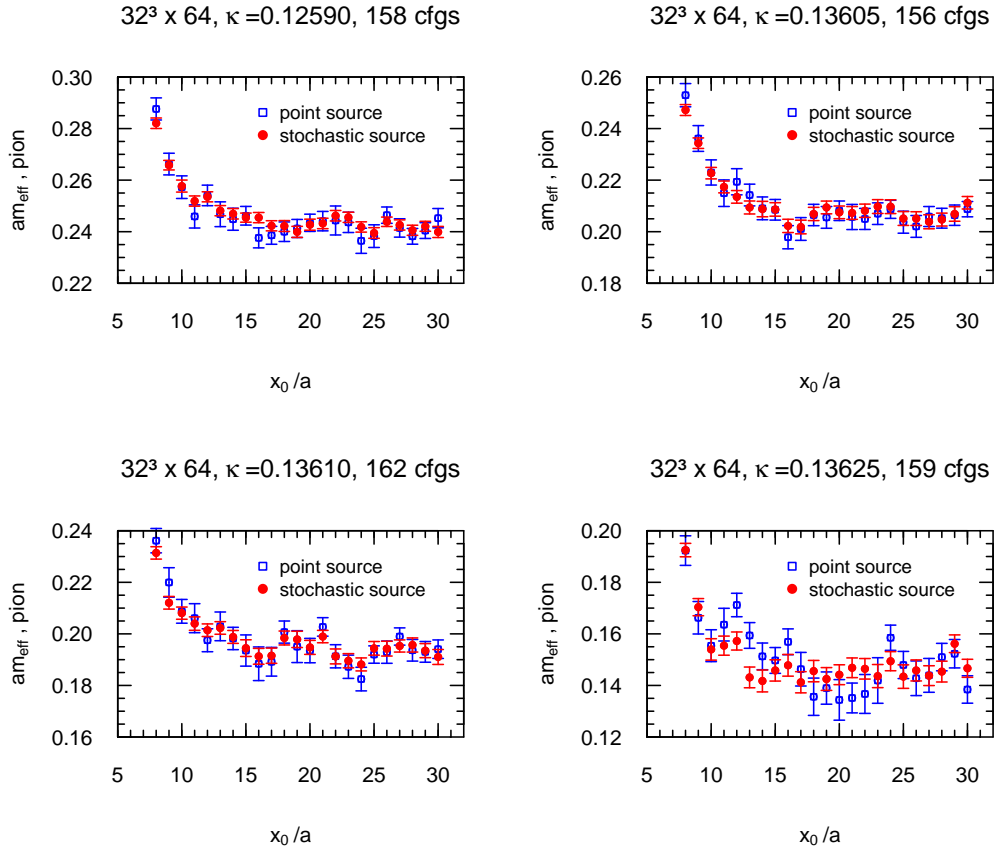


Figure 5: Effective pion mass plots for the ensembles $E_2 - E_5$ (from top left to bottom right). Illustrated are the results for the point source (blue squares) and the stochastic volume source (filled red circles) at fixed cost, i.e. for $N_r = 3$ hits.

B Effective mass plots: vector channel

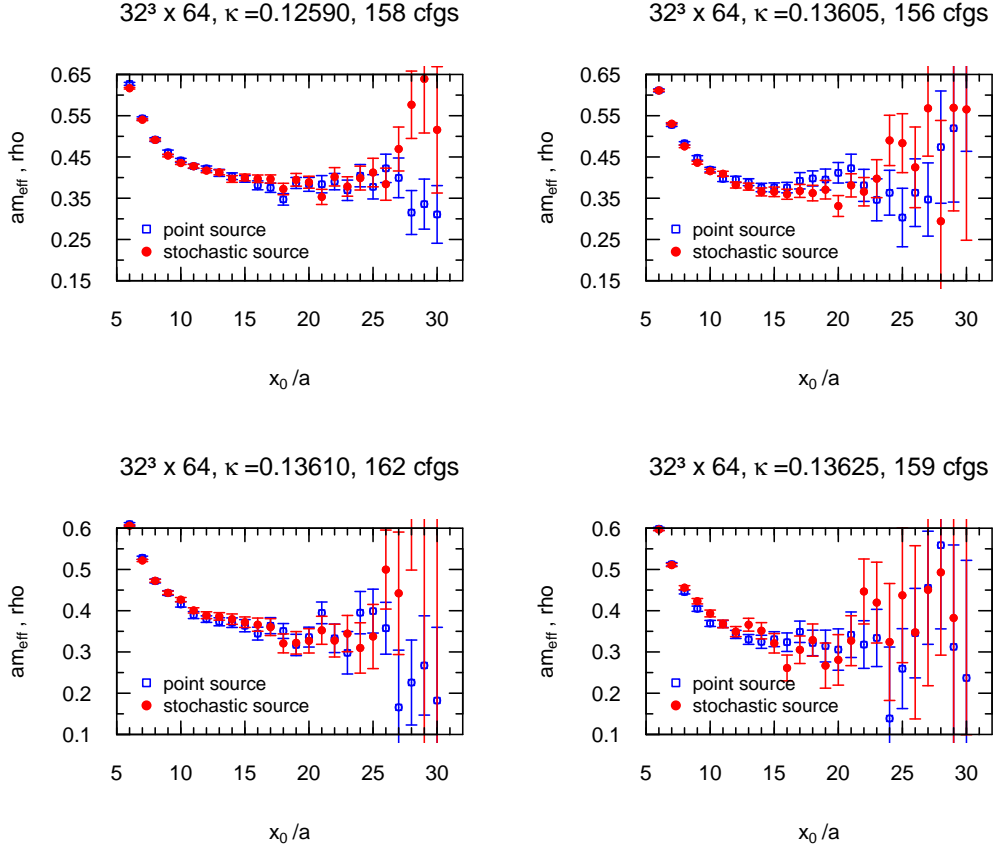


Figure 6: Effective rho meson mass plots for the ensembles $E_2 - E_5$ (from top left to bottom right). Illustrated are the results for the point source (blue squares) and the stochastic volume source (filled red circles) at fixed cost, i.e. for $N_r = 3$ hits.

References

- [1] S. Bernardson, P. McCarty and C. Thron, Comput. Phys. Commun. **78** (1993) 256.
- [2] S.J. Dong and K.F. Liu, Phys. Lett. B **328** (1994) 130, hep-lat/9308015.
- [3] G.M. de Divitiis, R. Frezzotti, M. Masetti and R. Petronzio, Phys. Lett. B **382** (1996) 393 hep-lat/9603020.
- [4] C. Michael and J. Peisa [UKQCD Collaboration], Phys. Rev. D **58** (1998) 034506, hep-lat/9802015.
- [5] M. Foster and C. Michael [UKQCD Collaboration], Phys. Rev. D **59** (1999) 074503, hep-lat/9810021.

- [6] T. Struckmann *et al.* [T χ L Collaboration], Phys. Rev. D **63** (2001) 074503, hep-lat/0010005.
- [7] A. O’Cais, K.J. Juge, M.J. Peardon, S.M. Ryan and J.I. Skullerud [TrinLat Collaboration], Nucl. Phys. B (Proc. Suppl.) **140** (2005) 844, hep-lat/0409069.
- [8] J. Foley, K.J. Juge, A. O’Cais, M. Peardon, S.M. Ryan and J.I. Skullerud, Comput. Phys. Commun. **172** (2005) 145, hep-lat/0505023.
- [9] C. McNeile and C. Michael [UKQCD Collaboration], Phys. Rev. D **73** (2006) 074506, hep-lat/0603007.
- [10] R. Frezzotti, V. Lubicz and S. Simula, Phys. Rev. D **79** (2009) 074506, arXiv:0812.4042.
- [11] P.A. Boyle, A. Jüttner, C. Kelly and R.D. Kenway, JHEP **0808** (2008) 086, arXiv:0804.1501.
- [12] J. Bulava, R. Edwards, C. Morningstar, PoS **LATTICE2008** (2008) 124, arXiv:0810.1469.
- [13] P.F. Bedaque, Phys. Lett. B **593** (2004) 82; G.M. de Divitiis, R. Petronzio, N. Tantalo, Phys. Lett. B **595** (2004) 408; C.T. Sachrajda, G. Villadoro, Phys. Lett. B **609** (2005) 73; B.C. Tiburzi, Phys. Lett. B **617** (2005) 40; P.F. Bedaque, J-W. Chen, Phys. Lett. B **616** (2006) 208; J.M. Flynn, A. Jüttner, C.T. Sachrajda, Phys. Lett. B **632** (2006) 313.
- [14] P. Boucaud *et al.* [ETM collaboration], Comput. Phys. Commun. **179** (2008) 695, arXiv:0803.0224.
- [15] K. Jansen, C. Michael and C. Urbach [ETM Collaboration], Eur. Phys. J. C **58** (2008) 261, arXiv:0804.3871.
- [16] P.A. Boyle *et al.*, JHEP **0807** (2008) 112, arXiv:0804.3971.
- [17] <http://twiki.cern.ch/twiki/bin/view/CLS/WebHome>
- [18] M. Lüscher, Comput. Phys. Commun. **165** (2005) 199, hep-lat/0409106; JHEP **0712** (2007) 011, arXiv:0710.5417.
- [19] Y. Saad, *Iterative methods for sparse linear systems*, 2nd edition (SIAM, 2003); A. Quarteroni and A. Valli, *Domain decomposition methods for partial differential equations* (Oxford University Press, 1999).
- [20] S. Duane, A.D. Kennedy, B.J. Pendleton and D. Roweth, Phys. Lett. B **195** (1987) 216.
- [21] J.C. Sexton and D.H. Weingarten, Nucl. Phys. B **380** (1992) 665.
- [22] K. Jansen and R. Sommer [ALPHA collaboration], Nucl. Phys. B **530** (1998) 185 [Erratum-ibid. B **643** (2002) 517], hep-lat/9803017.
- [23] M. Lüscher, Comput. Phys. Commun. **156** (2004) 209, hep-lat/0310048.
- [24] S. Capitani, M. Della Morte, E. Endreß, A. Jüttner, B. Knippschild, H. Wittig and M. Zambrana, PoS **LAT2009** (2009) 095, arXiv:0910.5578; B.B. Brandt *et al.*, PoS **LAT2010** (2010) 164, arXiv:1010.2390.

- [25] S. Capitani, M. Della Morte, G. von Hippel, B. Knippschild and H. Wittig, PoS **Lattice 2011** (2011) 145, arXiv:1110.6365 [hep-lat].
- [26] L. Del Debbio, L. Giusti, M. Lüscher, R. Petronzio, N. Tantalo, JHEP **0702** (2007) 082, hep-lat/0701009v1.
- [27] B.A. Berg, Comput. Phys. Commun. **69** (1992) 7.
- [28] B.B. Brandt *et al.*, Eur. Phys. J. ST **198** (2011) 79, arXiv:1106.1554 [hep-lat]; B.B. Brandt, A. Jüttner and H. Wittig, arXiv:1109.0196 [hep-lat].